

The compressibility of water between 0 and 100 atm is determined by this equation as follows: the difference in slopes from the mercury and mercury-water curves, b , is $(12.490 - 9.662) \times 10^{-5}$, or 2.828×10^{-5} . Also, $\beta_{Hg} = 4.009 \times 10^{-6}$ atm $^{-1}$, $P_1 = 1469.6$ psia, $W = 0.7303$ g, $D = 0.9970$ g/cm 3 , and $\rho = 13.5340$ g/cm 3 . On substituting these values in the compressibility equation, one obtains $\beta_{water} = 45.91 \times 10^{-6}$ atm $^{-1}$. This compares favorably with Kretschmar's value of 46.13×10^{-6} atm $^{-1}$. The values for the compressibilities of pure n-propyl nitrate and n-butyl nitrate at 25°C along with other pertinent properties are tabulated in Table 1.

References

¹ Kretschmar, G. G., "The isothermal compressibilities of some rocket propellant liquids, and the ratio of the two specific heats," *Jet Propulsion* 24, 175-179 (1954).

² Richards, T. W. and Stull, W. N., "New method for determining compressibility," *Carnegie Inst. of Washington, Rept.* 7 (1903).

Compressibility Effects of Slender Bodies Entering Vertically into Water

INGE L. RYHMING*

General Dynamics/Astronautics, San Diego, Calif.

THIS note discusses vertical entry of slender bodies into water at very high speeds, in which the effect of compressibility of the water may not be neglected. Recently the incompressible counterpart of this problem was treated by Moran.¹

If the entering body is slender, the gasdynamic equations may be linearized, resulting in the wave equation for the velocity potential ϕ in the water²

$$(1/c^2)\phi_{tt} - \phi_{xx} = \phi_{rr} + (1/r)\phi, \quad (1)$$

where c is the speed of sound in the water, t the time, and (x,r) axisymmetric coordinates fixed with the free-water surface and the positive x -axis directed upward. Furthermore, by linearizing the free-surface boundary condition³ and neglecting the effect of the Froude number (since the speed of entry U is large), the boundary condition on the free surface takes the form¹

$$\phi = 0 \quad \text{on} \quad x = 0 \quad (2)$$

A body of revolution moving along the x -axis can be represented by a distribution of sources that vary in time along the axis of flight. The potential of these sources is represented by an integral (expressing the superposition of spherical waves emanating from each point on the axis) of the retarded values of the source strength $S(x,t)$ ⁴

$$-4\pi\phi(x,r,t) = \int_{-\infty}^{+\infty} \frac{S\{\xi,t - (1/c)[(x-\xi)^2 + r^2]^{1/2}\}}{[(x-\xi)^2 + r^2]^{1/2}} d\xi \quad (3)$$

The source strength is zero outside the body so that the integral Eq. (3) covers only those values of ξ which are common to the flight path and the surface of the retrograde Mach cone

Received by IAS May 24, 1962. This research was done for the Hydrodynamics Section of General Dynamics/Convair under Contract No. 60-0494-d. The author would like to thank Julian D. Cole for suggesting this approach to the problem and for many stimulating discussions during the course of this study.

* Staff Scientist, Space Science Laboratory.

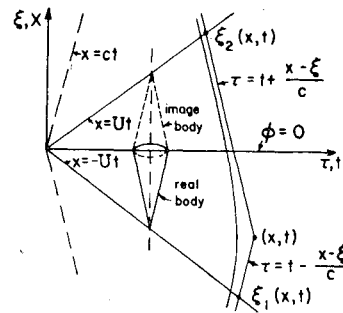


Fig. 1 Flight-path diagram for the entry problem

$\tau = t - [(x - \xi)^2 + r^2]^{1/2}(1/c)$. The flight-path diagram (the x,t -diagram), because of Eq. (2), will be represented as in Fig. 1. To satisfy Eq. (2), one uses the principle of source images and obtains the following condition expressing antisymmetry in x : $S(x,t) = -S(-x,t)$. The traces of the body nose and its x,t -diagram image in the will be the lines $x = -Ut$ and $x = Ut$.

There will be interest in the pressure on the body surface ($x < 0$), and since the body is slender the potential expression in Eq. (3) may be expanded for small r -values. There will then be an integral for the recent past ξ_1 to ξ_2 (Fig. 1) where $\xi_1(x,t)$ and $\xi_2(x,t)$ are the intersections of the retrograde Mach cone (r small $\rightarrow 0$) with the symmetric flight-path curves. The procedure of expanding Eq. (3) for small r is given in Ref. 4, where the resulting asymptotic expansion of the source distribution near the axis is also given. The source strength $S(x,t)$ is determined by the requirement that the flow be tangential at the surface. Within linearized theory, one obtains⁴ $S(x,t) = \partial A(x,t)/\partial t$, where $A(x,t)$ is the cross-sectional area distribution of the body as a function of x and t .

The theory just outlined will be used to calculate the pressure distribution on a cone entering the water with a constant speed $U < c$. The function $S(x,t)$ becomes, then,

$$S(x,t) = 2\pi Uk^2(x + Ut), \quad (4a)$$

$$S(x,t) = -2\pi Uk^2(Ut - x), \quad (4b)$$

or

$$S(x,t) = 2\pi Uk^2\{(x + Ut)H(x + Ut)[1 - H(x)] - (Ut - x)H(x)[1 - H(x - Ut)]\} \quad (5)$$

where $k = \tan \theta_0$, θ_0 is the semiangle at the vertex of the cone, and $H(x)$ is the Heaviside unit step function. The two points ξ_1 and ξ_2 are given by $\xi_1 = -(Ut - Mx)/(1 + M)$, $\xi_2 = (Ut + Mx)/(1 + M)$ where $M = U/c$. Defining a pressure coefficient c_p as $(p - p_\infty)/(\rho U^2/2)$, where p_∞ is the pressure at the free surface, and assuming for the water that $p\rho^{-n} = \text{const}$, one obtains the usual linearized pressure formula

$$c_p = -(2/U^2)\phi_t - (1/U^2)\phi_r + \dots \quad (6)$$

By calculating c_p from Eq. (6), one obtains for $-Ut < x < 0$

$$c_p = k^2 \left[\log \frac{4x^2}{k^2(U^2t^2 - x^2)} - 1 \right] \quad (7)$$

As is seen from Eq. (7), there is no Mach-number effect on the c_p -distribution for the cone.

Next, a drag coefficient c_F is defined by (F = force on the body)

$$c_F = \frac{F}{1/2\rho U^2\pi(Utk)^2} = \frac{2}{(Ut)^2} \int_{-Ut}^0 c_p(Ut + x)dx \quad (8)$$

For the cone, one gets

$$c_F = 2k^2[\log(1/2k) - (1/2)] \quad (9)$$

Because of the suction region at the shoulder, the theory breaks down completely for cone angles $\theta_0 > 16.9^\circ$, where c_F becomes negative.

The compressibility effects will be noticeable in the far flow field. To calculate these effects, recourse has to be made directly to the formula for ϕ in Eq. (3). For a large x and r value, the flight-path diagram will be the same as that shown in Fig. 1, but ξ_1 and ξ_2 will now be determined by the crossings of the retrograde trace of the retrograde Mach cone with the symmetric flight-path curves. In the far field, it will take a time $t = (1/c) (x^2 + r^2)^{1/2}$ before the first pressure pulse is felt in a given point (x,r) , and the pressure variation in this point will thereafter be given by the t -derivative of Eq. (3) with ξ_1 and ξ_2 determined as indicated above.

For the cone, the expression for $\phi_t(x,r,t)$ in the far field is very complicated and will not be given here. However, one gets a simple formula by letting $r \rightarrow 0$, which is

$$(c_p)_{r=0} = k^2 \log \frac{(1 - M^2)x^2}{x^2 - U^2t^2} \text{ for } \left(\frac{x}{c}\right)^2 \leq t^2 < \left(\frac{x}{U}\right)^2 \quad (10a)$$

$$(c_p)_{r=0} = 0 \text{ for } t^2 < \left(\frac{x}{c}\right)^2 \quad (10b)$$

Eqs. (10a) and (10b) give the time history of c_p for a fixed value of x .

References

- ¹ Moran, J. P., "The vertical water-exit and -entry of slender symmetric bodies," *J. Aerospace Sci.* **28**, 803-812 (1961).
- ² Oswatitsch, K., *Gas Dynamics* (Academic Press, Inc., New York, 1956), p. 541.
- ³ Milne-Thomson, L. M., *Theoretical Hydrodynamics* (Macmillan Co., New York, 1957), p. 376.
- ⁴ Cole, J. D., "Acceleration of slender bodies of revolution through sonic velocity," *J. Appl Phys* **26**, 322-326(1955).

Characteristics of Lateral Range during Constant-Altitude Glide

H. E. WANG* AND R. S. SKULSKY*
Aerospace Corporation, El Segundo, Calif.

THIS note presents some results of calculations of lateral range during a constant-altitude glide and discusses their characteristics. The constant-altitude glide is maintained by continuously rolling the vehicle about its velocity vector at a fixed angle of attack. The applicable equations of motion are

$$(2W/C_D A \rho)(dV/dt) = -gV^2 \quad (1)$$

$$V^2(L/D) \cos\phi = (2W/C_D A \rho)[1 - (V/V_s)^2] \quad (2)$$

$$\frac{d\psi}{dt} = \frac{L}{D} \frac{Vg \sin\phi}{(2W/C_D A \rho)} - \frac{Vg \cos\psi \tan\lambda}{V_s^2} \quad (3)$$

$$d\lambda/dt = Vg \sin\psi/V_s^2 \quad (4)$$

The symbol ϕ is the roll angle measured from the local vertical, ψ is the turn angle measured from the vehicle's original heading, λ is the ratio of the lateral range (measured from the original great circle) to the radius of the earth, and V_s is the orbital speed. Other symbols have their usual meaning. The first term on the right-hand side of Eq. (3) is proportional to the lateral aerodynamic force, whereas the second term is proportional to the so-called lateral centrifugal force, which accounts for the effect of the earth's curvature in the lateral direction. Equation (3) can be deduced from Eq. (60) of Ref. 5.

These equations have been solved on a digital computer by Skulsky,¹ and some of the results are shown in Fig. 1 for a

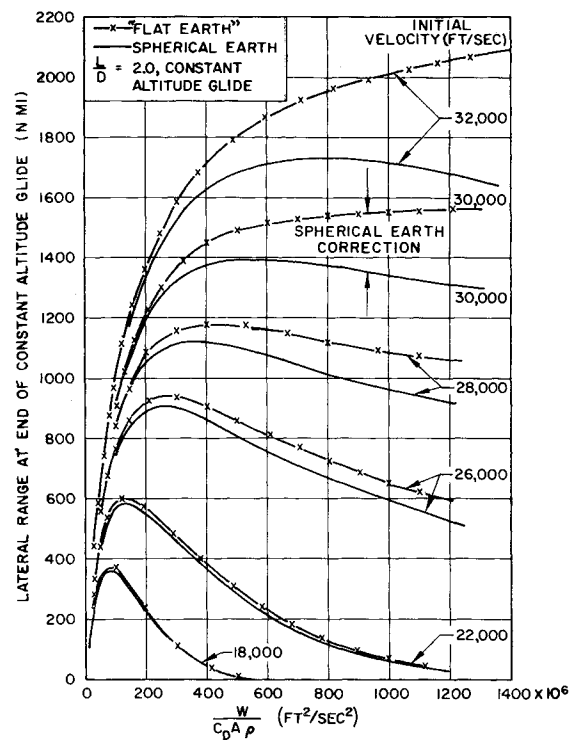


Fig. 1 Lateral range for various initial velocities and $W/C_D A \rho$

range of $W/C_D A \rho$ of practical interest. The lateral range presented is that obtained from the beginning of the constant-altitude glide at initial velocities indicated and an associated initial roll angle to the end of the glide, where the roll angle is zero. The results are for $L/D = 2$. Both the "flat-earth"[†] and spherical-earth calculations are presented.

It is well known that the lateral range during an equilibrium glide, keeping the vehicle at a constant roll angle and assuming a flat earth, is independent of $W/C_D A$ (see Ref. 2). This independence, however, does not hold for constant-altitude glides, as shown in Fig. 1. During a constant-altitude glide, the required roll angle at any instant is a function of $W/C_D A \rho$ and L/D . This leads to the $W/C_D A \rho$ dependence of the turn angle ψ and hence the lateral range. This can be seen readily by the substitution of Eqs. (1) and (2) into (3).

Figure 1 reveals that the lateral range, as a function of $W/C_D A \rho$, exhibits maxima in all of the spherical-earth calculations and in most of the "flat-earth" calculations. Since maxima occur in the "flat-earth" cases, it is concluded that these maxima result fundamentally from the lateral aerodynamic-force term and can be understood by examining the lateral aerodynamic force only. For a given initial velocity, the turn angle ψ decreases as $W/C_D A \rho$ increases, as indicated by Eqs. (2) and (3). On the other hand, the total flight time from the beginning to the end of the constant-altitude glide increases as $W/C_D A \rho$ increases; this is true at least for the lower end of $W/C_D A \rho$. The velocity reduction during this time decreases as $W/C_D A \rho$ increases. Although the lateral range, as given by Eq. (4), is the time integral of $V \sin\psi$ (g and V_s essentially are constant), a maximum occurs as $W/C_D A \rho$ increases because of less velocity reduction, higher total time, and lower $\sin\psi$.

The data of Fig. 1 also show that the magnitude of lateral range is not always a satisfactory criterion for determining the validity of neglecting the spherical-earth correction. It is observed from Fig. 1 that for low values of $W/C_D A \rho$ the lateral range obtained by assuming a "flat earth" agrees fairly well with the spherical earth results, regardless of the magnitude of the lateral range and the initial velocity. The

[†] In the flat-earth calculations, only the lateral centrifugal force was neglected.